

Fluorescent macrocyclic chemosensor for Zn(II) detection at alkaline pH values

Gianluca Ambrosi, Mauro Micheloni, Daniele Paderni, Mauro Formica, Luca Giorgi & Vieri Fusi

To cite this article: Gianluca Ambrosi, Mauro Micheloni, Daniele Paderni, Mauro Formica, Luca Giorgi & Vieri Fusi (2020): Fluorescent macrocyclic chemosensor for Zn(II) detection at alkaline pH values, *Supramolecular Chemistry*, DOI: [10.1080/10610278.2020.1713324](https://doi.org/10.1080/10610278.2020.1713324)

To link to this article: <https://doi.org/10.1080/10610278.2020.1713324>

 [View supplementary material](#) 

 Published online: 14 Jan 2020.

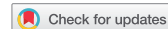
 [Submit your article to this journal](#) 

 Article views: 6

 [View related articles](#) 

 [View Crossmark data](#) 

ARTICLE



Fluorescent macrocyclic chemosensor for Zn(II) detection at alkaline pH values

Gianluca Ambrosi, Mauro Micheloni, Daniele Paderni, Mauro Formica, Luca Giorgi and Vieri Fusi

Department of Pure and Applied Sciences, University of Urbino, Urbino, Italy

ABSTRACT

The new macrocyclic ligand **L** (28,29-dimethoxy-27-oxa-8,11,14,17,25,26-hexaazatetracyclo [22.2.1.1(2,6).1(19,23)]nonacosa-2,4,6(28),19,21,23(29),24,26(1)-octaene) has been synthesised. It contains a tetramine chain and the 2,5-bis(2-methoxy-3-methyl-phenyl)-1,3,4-oxadiazole (PPD-OMe) chromophore, acting as coordinating and sensing units, respectively.

The fluorescent emission of **L** depends on the pH being highly fluorescent at pH = 2 and not emitting from pH >10. The studies highlighted that **L** is a PET mediated emitting chemosensor, being the PET effect regulated by the degree of the tetraamine protonation.

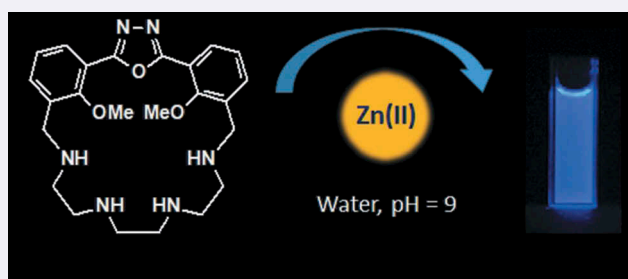
L coordinates metal ions (Cu(II), Zn(II) and Cd(II)) in water giving rise to an OFF-ON fluorescent response for the presence of Zn(II) ion thus signalling its presence in the medium. This response is particularly notable at pH = 9 allowing to extend the Zn(II) sensing also in the alkaline pH field.

ARTICLE HISTORY

Received 12 September 2019
Accepted 3 January 2020

KEYWORDS

Zinc sensor; Macrocyclic; 2,5-Diphenyl-1,3,4-oxadiazole; 5-Diphenyl-1; Fluorescence



Introduction

The development of new chemosensors is an attractive and continuous growing field of research due to its multiple applications ranging from the biological to the industrial ones.

They are molecular systems able to respond to the presence of a target substance by physico-chemical measurable responses which, as a first application, highlights the presence of the target in a context. In addition of this, they are useful for further and appealing uses ranging from the analytical quantification of the target to be the base of logic gates as well as to map and trace the target in an environment up to the imaging for medical applications; in any cases, their response to an external stimulus makes them a suitable base for sensor devices (1–7).

In this light, there is a continuous research in designing chemosensors able to respond to selected external stimuli, as could be the presence of a specific substrate, even more

selective both in molecular recognition and related response.

Among the physico-chemical signals exhibited by the system as a response to the stimulus, the fluorescence is one of the most appealing so most of the chemosensors are fluorescence-based. The fluorescence shows many advantages: the fluorescent emission of light is usually very sensitive being able to change with the presence of the substrate even at very low concentration; the related measurements are of low cost, easily performed, and versatile, offering subnanometer spatial resolution with submicron visualisation and submillisecond temporal resolution (8–14).

In any case, all chemosensors exploit inputs induced by the environment, as the presence of a selected substrate; this, in the case of the fluorescent ones, induces modification of the fluorescent emission obtaining information about it, leading also the development of the technology based on fluorescent probes. Nevertheless, the principles on which the fluorescence and thus the

CONTACT Luca Giorgi ✉ luca.giorgi@uniurb.it; Vieri Fusi ✉ vieri.fusi@uniurb.it Department of Pure and Applied Sciences, University of Urbino, P.zza Rinascimento 6, Urbino 61029, Italy

 Supplemental data for this article can be accessed [here](#).

© 2020 Informa UK Limited, trading as Taylor & Francis Group

systems developed performance remaining the same and it is the applications that have gone forward (15).

Metal ions and their selective recognition and sensing are one of the most common targets of chemosensors; they can be found in very different environmental compartments ranging from the soil to water to a biological apparatus as well as they can be found in different oxidation states (16–18).

From the biological point of view, zinc is an ubiquitous and multifunctional metal in human metabolism, being involved in the catalytic function of almost 300 enzymes. Zinc is present in all major biochemical pathways and it is essential for DNA metabolism and recognition by numerous proteins (19). The determination of the exact amount of zinc in living systems is still a stimulating challenge. In this context, the development of fluorescent chemosensors with a selective response towards Zn(II) in aqueous solution is important (20).

Considering this aspect, it is interesting to consider that zinc ion and related biological functions exert their functions at specific pH values or ranges. For example, carbonic anhydrase (CAs) is a class of zinc-based enzymes catalysing the reversible hydration of carbon dioxide in a two-steps conversion: carbon dioxide-hydrogencarbonate ion and an excess proton via the 'ping-pong' mechanism (21). The CO₂ hydration turnover rate depends on the pH and it is maximum, for example, for the human CA II enzyme at pH = 9 (about 10⁶ sec⁻¹) (22).

This is to say that the environment and, in this case, the pH is a variable to consider for the sensing response. In many cases, it is not only important to obtain a specific response to a substrate as a metal ion but to obtain it in a specific condition as the pH value.

In the recent years, we are interested in selective chemosensors for anions (23) and metal ions (24) and among them for the Zn(II) detection (25). Recently, we developed a specific fluorescent chemosensor for Zn(II) (**L1** in Chart 1), working at neutral pH (26). It is a fluorescent macrocyclic chemosensor formed by the tetraamine 1,4,7,10-tetraazadecane binding framework for metal ions and the 2,5-diphenyl-1,3,4-oxadiazole (PPD) fluorophore as sensing unit. **L1** is able to vary the fluorescent emission as a function of pH as well as to respond to Zn(II) at neutral pH value. In the PPD fluorophore unit, the 1,3,4-oxadiazole rings (ODA) plays the central role on which to build the conjugated PPD system. It is to highlight that ODA-derived compounds in which ODA results conjugated with further aromatic rings showed interesting applications in biological (27) and material fields (28).

Following these results, other chemosensor based on the PPD sensing unit has been synthesised and studied obtaining interesting fluorescent sensing response (29).

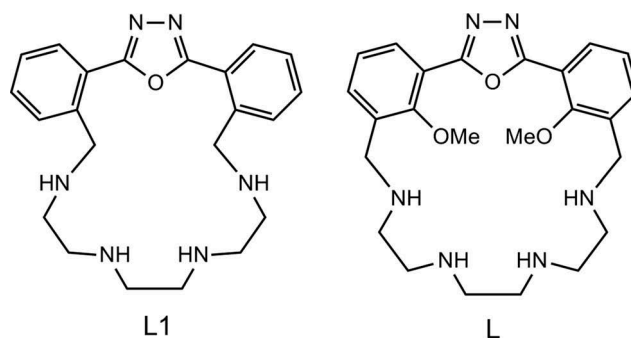


Chart 1. Schematic drawing of ligands **L1** and **L**.

In order to extend the knowledge about the oxadiazole-containing fluorescent systems inserted in a polyamine macrocyclic skeleton, we have developed the 2,5-bis(2-methoxy-3-methyl-phenyl)-1,3,4-oxadiazole sensing unit (PPD-OMe) suitable to be inserted, after adapt functionalization and cyclisation, in a macrocyclic skeleton. In this paper, PPD-OMe has been cyclised together with the same tetraamine (1,4,7,10-tetraazadecane) of **L1** obtaining the new chemosensor **L** (Chart 1).

In this paper, the synthesis of **L** (28,29-dimethoxy-27-oxa-8,11,14,17,25,26-hexaazatetracyclo[22.2.1.1(2,6).1(19,23)]nonacosa-2,4,6(28),19,21,23(29),24,26(1)-octaene) together with its fluorescent sensing properties towards H⁺ and selected transition metal ions were reported.

Experimental

Synthesis

All chemicals were purchased from Aldrich, Fluka and Lancaster in the highest quality commercially available. 1,4,7,10-tetrakis(4-methylbenzenesulfonyl)-1,4,7,10-tetraazadecane was prepared as reported (30).

Methyl 2-methoxy-3-methylbenzoate (2)

Dimethylsulfate (36.1 cm³, 48.0 g, 381 mmol) was added dropwise to a suspension of **1** (20.0 g, 131 mmol) and K₂CO₃ (52.7 g, 381 mmol) in 250 cm³ of anhydrous acetone. The mixture was refluxed further 16 h, subsequently was cooled to room temperature and filtered to remove the insoluble salts. The solvent was removed under reduced pressure, the residue was re-suspended in water (1000 cm³) and extracted with ethyl acetate (3 x 250 cm³). The organic phases were collected, washed with brine (250 cm³), dried over MgSO₄ and evaporated under reduced pressure obtaining the product (**2**) as a brown oil (22.2 g, 94%). MS m/z (ESI): 181.1 (M + H⁺); ¹H NMR: (400 MHz, CDCl₃) δ (ppm): 2.32 (3H, s), 3.83 (3H,

s), 3.91 (3H, s), 7.05 (1H, t, $J = 7.5$ Hz), 7.34 (1H, dd, $J_1 = 7.5$ Hz, $J_2 = 1.6$ Hz), 7.63 (1H, dd, $J_1 = 7.5$ Hz, $J_2 = 1.6$ Hz). ^{13}C NMR (CDCl_3) δ (ppm): 16.2, 52.3, 61.6, 123.7, 124.7, 129.3, 132.9, 135.3, 158.5, 167.1.

2-Methoxy-3-methylbenzhydrazide (3)

Hydrazine monohydrate (9.06 g, 181 mmol) was carefully added to a solution of ester **2** (10.0 g, 55.5 mmol) in 100 cm^3 of methanol and refluxed for 24 h under nitrogen. Subsequently, the mixture was cooled to room temperature then concentrated under reduced pressure to one-third of the initial volume, then poured under stirring into cold water (500 cm^3). The resulting white precipitate was filtered off, washed with cold water and dried under reduced pressure affording **3** as a white solid (8.9 g, 89%). MS m/z (ESI): 181.1 ($\text{M} + \text{H}^+$); ^1H NMR: (400 MHz, CDCl_3) δ (ppm): 2.33 (3H, s), 3.77 (3H, s), 7.13 (1H, t, $J = 7.6$ Hz); 7.31 (1H, dd, $J_1 = 7.6$ Hz, $J_2 = 1.5$ Hz), 7.89 (1H, dd, $J_1 = 7.6$ Hz, $J_2 = 1.5$ Hz).

2-Methoxy-3-methylbenzoic acid (4)

15% w/w aqueous NaOH (50 cm^3) was carefully added to a refluxing solution of ester **2** (10.0 g, 55.5 mmol) in 100 cm^3 of methanol. Subsequently, the mixture was cooled to room temperature then concentrated under reduced pressure to one-third of the initial volume, adjusted to pH = 7 by careful addition of 10 M HCl then poured under stirring into cold water (500 cm^3). The resulting white precipitate was filtered off, washed with cold water and dried under reduced pressure affording **4** as a white solid (8.3 g, yield 90%). MS m/z (ESI): 167.1 ($\text{M} + \text{H}^+$); ^1H NMR: (400 MHz, CDCl_3) δ (ppm): 2.83 (3H, s), 3.93 (3H, s), 7.18 (1H, t, $J = 7.7$ Hz), 7.43 (1H, br d, $J = 7.7$ Hz), 7.96 (1H, dd, $J_1 = 7.7$, $J_2 = 1.8$ Hz). ^{13}C NMR (CDCl_3) δ (ppm): 16.1, 62.3, 122.1, 125.2, 130.9, 131.7, 137.1, 157.9, 166.4.

2,5-bis(2-methoxy-3-methylphenyl)-1,3,4-oxadiazole (6)

A suspension of **4** (5 g, 30 mmol) in 150 cm^3 of phosphorus oxychloride (POCl_3) was refluxed under nitrogen until complete dissolution (about 3 h) forming the intermediate acyl-chloride **5**. The solution containing **5** was freshly used without purification cooling it at 0–5°C in an ice bath, then **3** (5.4 g, 30 mmol) was slowly added. The resulting solution was warmed to room temperature and stirred for 2 h, then refluxed overnight. After cooling the yellow solution was poured in 2 dm^3 of an ice/water mixture and carefully neutralised adding solid sodium carbonate (Na_2CO_3) in a small portion until the crude product **6** precipitates. The solid sample was filtered off, washed with cold water, collected and dried under vacuum at 60°C. Pure product **6** was obtained by flash-chromatography on silica gel using chloroform (CHCl_3) as

eluent (obtained 6.9 g, yield 74%). MS m/z (ESI): 311.1 ($\text{M} + \text{H}^+$); ^1H NMR: (400 MHz, CDCl_3) δ (ppm): 2.41 (6H, s), 3.91 (6H, s), 7.18 (2H, t, $J = 7.6$ Hz), 7.40 (2H, dd, $J_1 = 7.6$ Hz, $J_2 = 1.2$ Hz), 7.91 (2H, dd, $J_1 = 7.6$ Hz, $J_2 = 1.2$ Hz). ^{13}C NMR (CDCl_3) δ (ppm): 16.1, 61.2, 118.0, 124.3, 128.0, 133.1, 134.7, 157.2, 163.2.

2,5-bis(3-bromomethyl-2-methoxyphenyl)-1,3,4-oxadiazole (7)

Compound **6** (2.0 g, 6.4 mmol), N-bromosuccinimide (2.4 g 13.4 mmol), and 2,2'-azobis(2-methylpropionitrile) (0.1 g, 0.6 mmol) were dissolved in 100 cm^3 of CCl_4 under nitrogen. The reaction was stirred under reflux for 24 h and then cooled and filtered and the solvent removed under reduced pressure. The crude product was washed with methanol (5 x 25 cm^3) and dried, giving **7** as a yellow solid (1.9 g, 63%). MS m/z (ESI): 467.0 ($\text{M} + \text{H}^+$); ^1H NMR: (400 MHz, CDCl_3) δ (ppm): 4.05 (6H, s), 4.67 (4H, s), 7.30 (2H, t, $J = 7.6$ Hz), 7.64 (2H, dd, $J_1 = 7.6$ Hz, $J_2 = 1.6$ Hz), 8.06 (2H, dd, $J_1 = 7.6$ Hz, $J_2 = 1.6$ Hz). ^{13}C NMR (CDCl_3) δ (ppm): 26.9, 62.7, 118.3, 125.0, 130.9, 133.5, 135.0, 157.2, 163.2.

28,29-dimethoxy-8,11,14,17-tetrakis(4-methylbenzoylsulfonyl)-27-oxa-8,11,14,17,25,26-hexaazatetracyclo[22.2.1.1(2,6).1(19,23)]nonacosane-2,4,6(28),19,21,23(29),24,26(1)-octaene (9)

Over a period of 6 h, a solution of **8** (2.7 g, 3.6 mmol) in 150 cm^3 of anhydrous DMF was added to a suspension of **7** (1.7 g, 3.6 mmol) and K_2CO_3 (5.0 g, 36 mmol) in 250 cm^3 of anhydrous DMF, at 90°C under nitrogen. The reaction mixture was maintained at 90°C for further 12 h. Subsequently, the mixture was cooled to room temperature then concentrated under reduced pressure to one-third of the initial volume, then poured under stirring into cold water (1 dm^3). The resulting white precipitate was filtered off, washed with cold water, dried under vacuum and purified by flash-chromatography (silica gel, chloroform) obtaining **9** as white solid (1.7 g, 44%). MS m/z (ESI): 1069.3 ($\text{M} + \text{H}^+$); ^1H NMR: (400 MHz, CDCl_3) δ (ppm): 2.40 (6H, s), 2.46 (6H, s), 3.08 (4H, br t, $J = 7.5$ Hz), 3.26 (4H, s), 3.35 (4H, br t, $J = 7.5$ Hz), 3.61 (6H, s), 4.49 (4H, s) 7.19 (4H, d, $J = 8.4$ Hz), 7.28 (2H, t, $J = 7.6$ Hz), 7.36 (4H, d, $J = 8.0$ Hz), 7.48 (4H, d, $J = 8.0$ Hz), 7.60 (2H, dd, $J_1 = 7.6$ Hz, $J_2 = 1.6$ Hz), 7.77 (4H, d, $J = 8.4$ Hz), 8.05 (2H, dd, $J_1 = 7.6$ Hz, $J_2 = 1.6$ Hz). ^{13}C NMR (CDCl_3) δ (ppm): 21.5, 21.6, 45.7, 46.1, 47.5, 48.4, 63.2, 117.8, 125.3, 127.2, 127.3, 129.7, 129.9, 131.0, 131.7, 135.0, 136.0, 137.0, 143.6, 157.2, 164.0.

28,29-dimethoxy-27-oxa-8,11,14,17,25,26-hexaazatetracyclo[22.2.1.1(2,6).1(19,23)]nonacosane-2,4,6(28),19,21,23(29),24,26(1)-octaene (L)

Macrocycle **9** (1.7 g, 1.6 mmol) and phenol (3.6 g, 38.3 mmol) were dissolved in $\text{HBr}/\text{CH}_3\text{COOH}$ (33%, 40 ml). The

solution was stirred at 90°C for 24 h. The resulting suspension was filtered and washed with CH₂Cl₂ several times. The solid obtained was recrystallised from cold water/48% aqueous HBr mixture to give **L**.4HBr as a white solid. The hydrobromide salt was dissolved in water (50 cm³), 25% NaOH aqueous solution was carefully added until pH > 11 and the resulting alkaline solution was extracted with CH₂Cl₂ (3 x 25 cm³). The organic phases were collected, washed with brine (250 cm³), dried over MgSO₄ and evaporated under reduced pressure obtaining the **L** as a bright yellow solid (470 mg, 65%). MS m/z (ESI): 453.5 (M + H⁺); ¹H NMR: (400 MHz, CDCl₃, 25°C) δ (ppm): 2.83 (12H, m), 3.76 (6H, s), 3.88 (4H, s), 7.26 (2H, t, *J* = 7.6 Hz), 7.44 (2H dd, *J*₁ = 7.6 Hz, *J*₂ = 1.6 Hz), 7.99 (2H dd, *J*₁ = 7.6 Hz, *J*₂ = 1.6 Hz). ¹³C NMR (CDCl₃) δ (ppm): 47.6, 49.2, 49.5, 49.7, 62.4, 118.0, 124.8, 130.6, 134.3, 134.6, 157.8, 164.1. Anal. for C₂₄H₃₂N₆O₃: Calcd C 63.70, H 7.13, N 18.57; Found C 63.9, H 7.4, N 18.4.

UV-Vis and fluorescence spectra

UV-Vis absorption spectra were recorded at 298.1 K on a Varian Cary-100 spectrophotometer equipped with a temperature control unit. Fluorescence emission spectra were recorded at 298.1 K on a Varian Cary-Eclipse spectrofluorimeter and the spectra are uncorrected. The fluorescence quantum yields of the free ligand and of its complexes (Φ_f) were determined by comparing the integrated fluorescence spectra of the sample with 2,2'-biphenol in acetonitrile ($\Phi_f = 0.29$) (31).

Elemental analyses

Elemental analyses were performed with a Thermo Finnigan Flash 1112 EA CHN analyser, mass spectra (MS-ESI) were acquired with a Waters Micromass ZQ mass spectrometer.

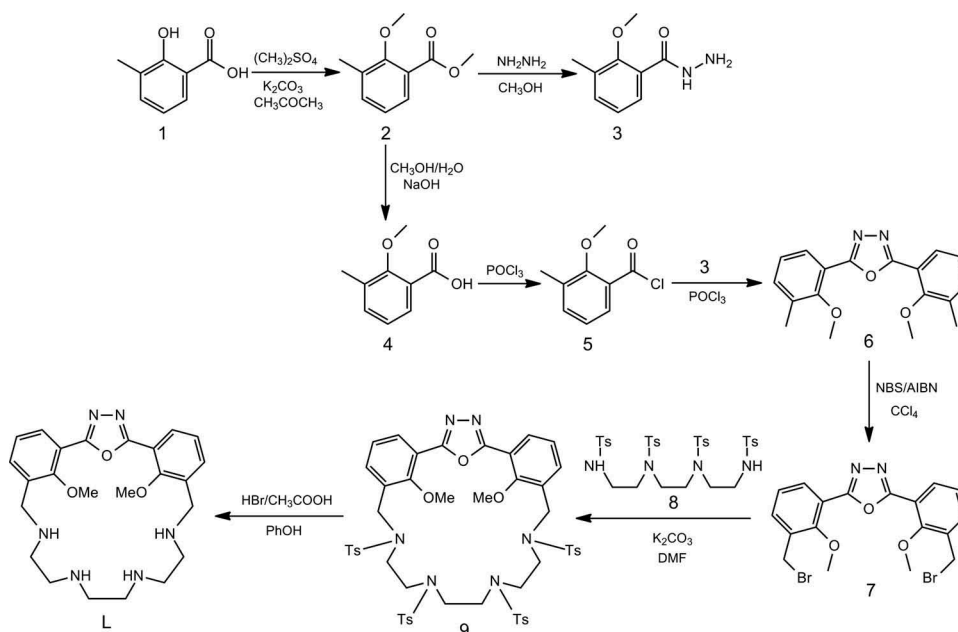
NMR studies

¹H- and ¹³C-NMR spectra were recorded on a Bruker Avance 400 instrument, operating at 400.13 and 100.61 MHz, respectively, and equipped with a variable temperature controller. The temperature of the NMR probe was calibrated using 1,2-ethandiol as calibration sample. For the spectra recorded in CDCl₃, the ¹H and ¹³C peak positions are reported with respect to the residual solvent. Chemical shifts (δ scale) are reported in parts per million (ppm values) and coupling constants (*J* values) are given in hertz (Hz). ¹H-¹H and ¹H-¹³C correlation experiments were performed to assign the signals.

Results and discussion

Synthesis

The synthetic pathway used to obtain the ligand **L** is depicted in Scheme 1. The heteroaromatic scaffold 2,5-bis(3-bromomethyl-2-methoxyphenyl)-1,3,4-oxadiazole **7** was synthesised by radicalic bromination with NBS of its precursor 2,5-bis(2-methoxy-3-methylphenyl)-1,3,4-oxadiazole **6**, obtained by condensation of



Scheme 1. Synthesis of ligand **L**.

hydrazide **3** with carboxylic acid **4** in POCl_3 following a modified procedure reported by Mashraqui and co-workers (32). The reaction used to obtain the tosylated macrocycle **9**, a modification of the Richman-Atkins method (33), involves the cyclisation of the polytosylated polyamine **8** with 1 equivalent of 2,5-bis(3-bromo-methyl-2-methoxyphenyl)-1,3,4-oxadiazole **7**, in the presence of an alkaline carbonate base. The final compound **9** was obtained using a 1 + 1 cyclisation scheme and purified from the crude products by flash-chromatography. Finally, the desired ligand **L** was obtained from the cleavage of the tosyl groups by using hydrobromic acid in acetic acid at 90°C in the presence of an excess of phenol as scavenger. Noteworthy, in these conditions, the two methyl groups bound to the oxygen atoms of **L** do not undergo cleavage. The ligand **L** was further purified as hydrobromide salt by recrystallisation from cold water/48% aqueous HBr mixture, and extracted in strong alkaline conditions to obtain pure free **L**.

Acid-base behaviour

Spectrophotometric titration

UV-Vis absorption and fluorescence electronic spectra were performed in water/ethanol 99/1 mixed solvent at different pH values to obtain information about the role of the photoactive aromatic system in the acid-base behaviour of the ligand (Figure 1).

The absorption spectra of **L** show an absorption band centred at $\lambda_{\text{max}} = 280 \text{ nm}$; the form of the band and its λ_{max} are independent from the pH but, its molar absorptivity is slightly pH-dependent, ranging from $\epsilon = 16,800 \text{ dm}^3 \cdot \text{mol}^{-1} \cdot \text{cm}^{-1}$ at $\text{pH} = 1.7$ to $\epsilon = 21,400 \text{ dm}^3 \cdot \text{mol}^{-1} \cdot \text{cm}^{-1}$ at $\text{pH} = 12.0$ (Figure 1(a)).

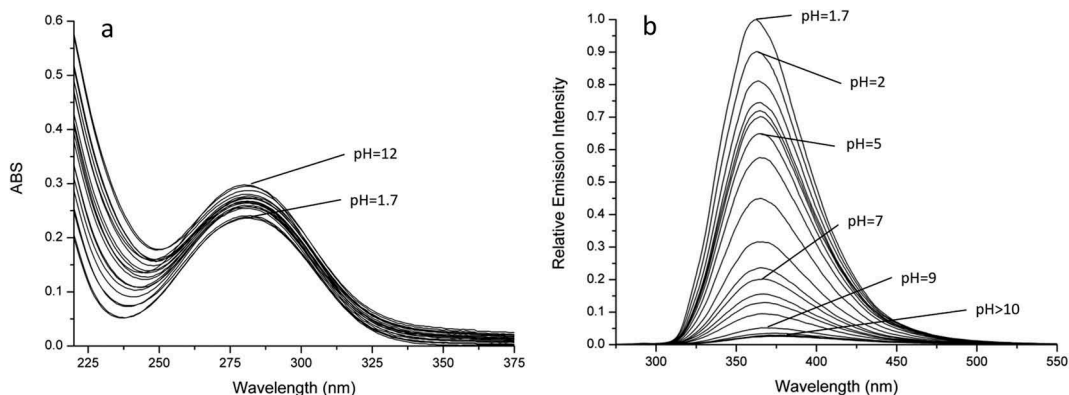


Figure 1. UV-Vis absorption (a) and emission (b) spectra of **L** recorded in water/ethanol 99/1 v/v solvent mixture in the pH range of 1.7 – 12.0. Experimental condition: $[\text{L}] = 1.5 \cdot 10^{-5} \text{ mol} \cdot \text{dm}^{-3}$, pH adjusted by adding HCl and NaOH aqueous solutions, emission spectra were acquired by exciting at $\lambda_{\text{ex}} = 280 \text{ nm}$ and they are corrected taking into account the variation in absorbance at the excitation wavelength.

The fluorescence spectra of **L** at different pH values were recorded upon exciting at $\lambda_{\text{ex}} = 280 \text{ nm}$; **L** resulted highly fluorescent in the acid pH range showing an emission band with a maximum emission at $\lambda_{\text{em}} = 362 \text{ nm}$ (fluorescence quantum yield $\Phi_f = 0.19$, Stokes-shift = 8090 cm^{-1}) (Figure 1(b)). Increasing the pH values, the fluorescence emission decreases reaching a maximum quenching level of 96.5% at $\text{pH} > 9$. This behaviour can be rationalised in terms of the excited state quenching due to photoinduced intramolecular electron transfer (PET) from the HOMO of the donor benzyl nitrogen atoms to the excited fluorophore moiety (34) occurring when the benzyl nitrogen shows a free lone pair.

Figure 2 reports the trend of the fluorescence emission at 362 nm as a function of pH; observing the trend

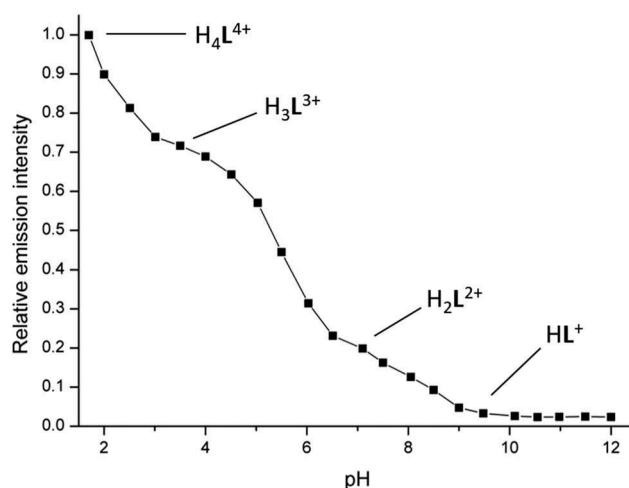


Figure 2. Trend of the emission intensity at 362 nm as a function of pH. Experimental conditions: $[\text{L}] = 1.5 \cdot 10^{-5} \text{ mol} \cdot \text{dm}^{-3}$, pH adjusted by adding HCl and NaOH aqueous solutions, $\lambda_{\text{ex}} = 280 \text{ nm}$, the emission intensity was corrected taking into account the drop in the absorbance at the excitation wavelength.

from pH = 1.7 to pH = 12.0, the curve exhibits a behaviour that can be related to three well separated deprotonation steps. Starting from pH = 1.7 to pH = 3 a drop of 23.5% of the emission intensity is observed, followed by a change in the slope of the curve, nearly a plateau, until pH = 4.5. From this pH to pH = 6.5 a further drastic drop of the fluorescence occurs, reaching a reduction of 75.5% with respect to the initial emission intensity, then a new change of the slope (plateau) can be observed up to pH = 7.5. In the pH range of 7.5–9.5 a last emission drop is observed reaching a quenching of 96.5% of the initial intensity that it is preserved until pH = 12. Based on the PET concept and taking into account the experience acquired studying other analogous ligands (26a,29a) we assumed that at pH = 1.7 all the aliphatic amine functions of **L** are protonated giving rise the H_4L^{4+} species in solution. The protonation of all the four aliphatic amine functions prevents the PET effect, gives rise the highest emitting species. The two drops of emission intensity, occurring up to pH = 3 (23.5% of quenching) and from pH 4.5 to pH = 6.5 (75.5% of quenching), suggest that two deprotonation steps occur affording the H_3L^{3+} and H_2L^{2+} species; the first prevailing from pH 3 to pH 4.5 and the latter from pH 6.5 to pH 7.5. The low residual emission observed can be justified by the involvement of the free lone pair on the unprotonated amine in a H-bond network with the protonated ones preventing, in part, the PET effect. The new drop of the emission after pH 7.5 is due to the third deprotonation process leading the formation of the HL^+ species; this deprotonation makes the benzylic amine lone pair fully available, making efficient the PET effect thus to completely quench the emission. The further deprotonation step, to give the neutral **L** species, occurred at higher alkaline pH values and it does not affect the emission because, as already

observed in a similar ligand (26a), an amine free lone pair close to the fluorophore unit is enough to quench the emission. Table 1 reports a possible disposition of protons in the ligand species.

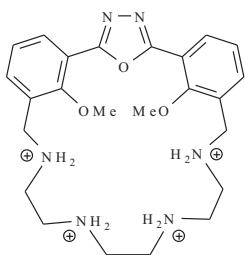
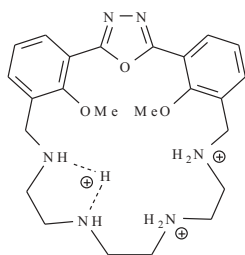
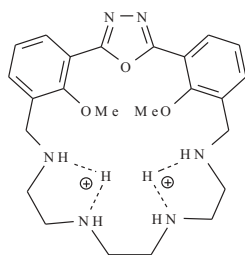
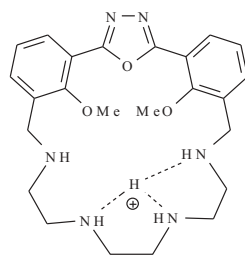
Metal ions complexation

Spectrophotometric studies

Spectrophotometric and spectrofluorimetric studies were carried out to evaluate the photochemistry of the PPD-OMe moiety upon coordination of metal ions by **L**. On the basis of the protonation studies, we established that the emission properties of the ligand is PET-regulated by the electron transfer from the lone pairs of the amine functions to the excited fluorophore; as a consequence, the coordination of a suitable metal ion into the macrocyclic moiety should affect the emission intensity by preventing or modulating this effect. Titration experiments were carried out by adding an aqueous solution of the selected metal ion as perchlorate salt to a solution of **L** dissolved in water/ethanol 99/1 v/v in the presence of HEPES buffer solution (10^{-3} mol·dm $^{-3}$) at pH = 7.0. Under these conditions, the addition of a transition metal ions such as Cu(II), Zn(II) and Cd(II) as perchlorate salts does not affect the absorption spectrum.

Observing the fluorescence emission of **L**, in these experimental conditions at pH = 7.0, the emission quantum yield Φ_f resulted 0.04 (λ_{ex} = 280 nm) with the maximum at 365 nm. By adding a selected metal ion it is possible to observe different emission behaviours depending on the metal ion added; in fact, the addition of Cu(II) ions totally quenched the emission while, the addition of the d^{10} metal ions Zn(II) and Cd(II) does not significantly affect the spectrum where only a very slight increase of the emission intensity was observed (Figure 3).

Table 1. Possible position of the protons in the **L** species based on fluorescence studies.

Relative emission intensity (percent)			
100%	76.5%	24.5%	3.5%
			
H_4L^{4+}	H_3L^{3+}	H_2L^{2+}	HL^+

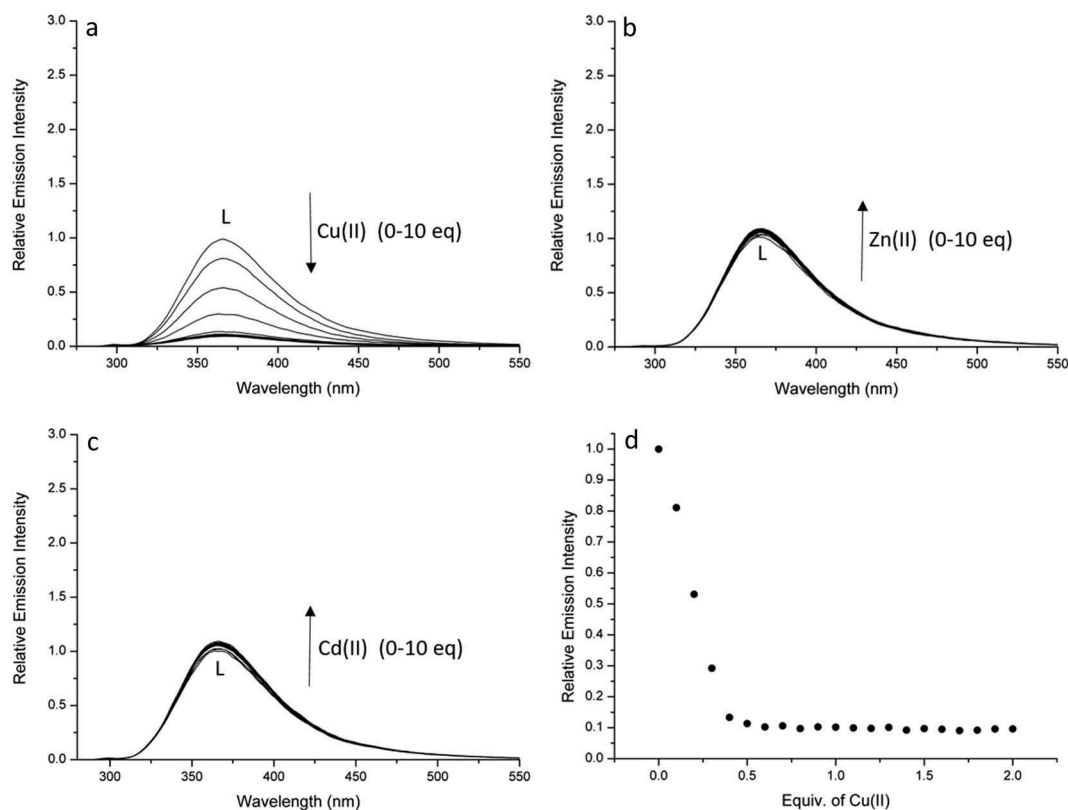


Figure 3. Fluorescence spectra of **L** ($\lambda_{\text{ex}} = 280 \text{ nm}$) registered in water/ethanol 99/1 v/v in the presence of HEPES buffer ($10^{-3} \text{ mol dm}^{-3}$) at pH = 7.0 by adding $\text{Cu}(\text{ClO}_4)_2$ (**a**), $\text{Zn}(\text{ClO}_4)_2$ (**b**) and $\text{Cd}(\text{ClO}_4)_2$ (**c**), trend of the emission intensity ($\lambda_{\text{em}} = 365 \text{ nm}$) as a function of the equivalents of Cu(II) added (**d**). ($[\text{L}] = 1.5 \cdot 10^{-5} \text{ mol dm}^{-3}$).

The change of the emission in the presence of Cu(II) indicates its coordination which leads to the quenching of the emission ascribed to the Chelation Quenching of Fluorescence effect (CHQF) determined by the paramagnetic character of this metal ion when it is coordinated by **L**. The titration with Cu(II) highlights that the fluorescence is completely quenched when 0.5 equiv. of Cu(II) was added (Figure 3(d)), suggesting the formation of 1:2 metal to ligand species, probably with $[\text{CuL}_2]^{2+}$ stoichiometry.

The slight increase of the emission intensity in the presence of Zn(II) or Cd(II) ions suggests that the two metal ions, although bound by **L** at this pH value, are not strongly coordinated by **L** (low stability constant) further suggesting that all the four amine functions were not strongly involved in the coordination in the presence of Zn(II) or Cd(II) ions. This does not completely prevent the PET effect to more switch on the emission as found with the analogous ligand **L1**, mainly with Zn(II), at the same pH value. In fact, in these experimental conditions, the increase of fluorescence due to Zn(II) and Cd(II) coordination is less than 5% and it is evident that such behaviour is not sufficient to justify the use of **L** as chemosensor at physiological pH at least for Zn(II) or Cd(II) ions.

However, the fluorescence experiments indicate that **L** coordinates the three metals but, observing the absorption spectra which remain always unvaried, the PPD-OMe fluorophore is not directly involved in the metal ion coordination thus meaning that the metal ions are coordinated only by the aliphatic polyamines moieties.

Considering the behaviour at pH = 7.0, we explored the best conditions for a valuable photochemical response to the presence of the metal ions in solution. In the case of Zn(II), the difference of the emission intensity of **L** alone or in the presence of 2 equivalents of Zn(II) in the 2–12 pH range has been measured. Figure 4(a) shows the fluorescence emission intensity of the 2Zn/**L** system and of **L** alone as a function starting from pH ≥ 6 because for pH < 6 the two emissions are coinciding. Figure 4(a) shows that no significant difference in the emission intensity was observed for pH values higher than 11.0 or lower than 7.0, thus meaning that both, the ligand and the metal complex, showed the same fluorescence in these pH ranges. Instead, the 2Zn/**L** system is more fluorescent with respect to the ligand alone in the pH range 7.0–10.5. The higher fluorescence of the 2Zn/**L** system than **L** in the range of pH 7–10.5, suggests the formation of a metal complex in which the Zn(II) coordination, almost partially, blocks the PET effect. At pH < 7

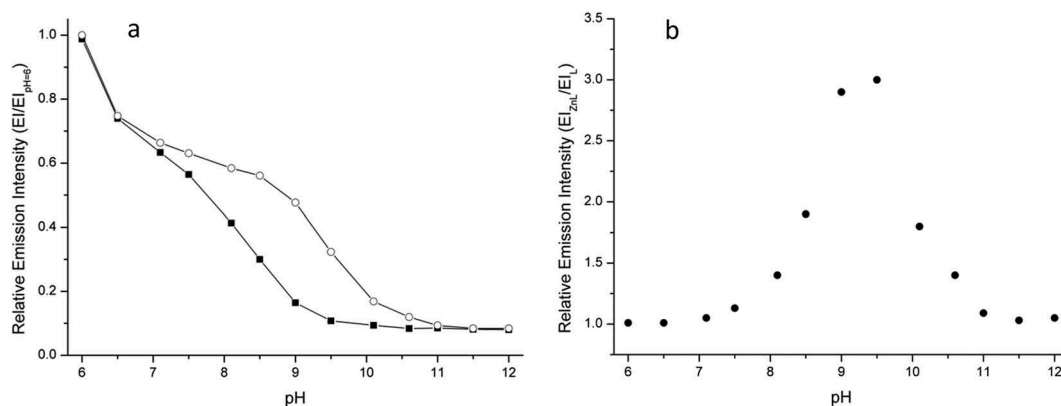


Figure 4. (a) Trend of the emission intensity as a function of pH (range 6–12) for free **L** (■) and 2Zn/**L** system (○). (b) trend of the fluorescent response of **L** to Zn(II) expressed as ratio between the emission intensities of the 2Zn/**L** system and free **L** as a function of pH (●). Experimental conditions: [**L**] = $1.5 \cdot 10^{-5}$ mol·dm⁻³, [Zn(II)] = $3.0 \cdot 10^{-5}$ mol·dm⁻³, pH adjusted by adding HCl and NaOH aqueous solutions, $\lambda_{\text{ex}} = 280$ nm, $\lambda_{\text{em}} = 365$ nm.

no differences was found between the emission intensities indicating that in acidic media Zn(II) ion is probably not coordinate by **L**, as well as in strong alkaline conditions (pH>10.5) the 2Zn/**L** system is not fluorescent probably due to the formation of hydroxo-species that, lengthening the Zn-N bonds, restores the PET effect.

Examining the fluorescent response of **L** to Zn(II) expressed as the ratio between the emission intensities of the 2Zn/**L** system and free **L** as a function of pH starting from pH≥6 (Figure 4(b)), it is evident that the best response can be obtained at pH = 9–9.5 in which, the presence of Zn(II) triplicates the emission intensity of **L**.

Similar experiment were performed with Cu(II) and Cd(II) metal ions founding not significant differences depending on the pH; in other words, while Cu(II) quenches completely the ligand, Cd(II) does not significantly affects the emission at all for pH≥6. The results are schematically reported in Figure 5.

In any case, as previously reported, the absorption spectra ascribed to the PPD-OMe chromophore was not perturbed in all range of pH examined with respect to free **L**, supporting the lack of its involvement in metal ion coordination.

Summarising the results, the best performance in terms of fluorescent response and selectivity has been reached at pH = 9, where the emission quantum yield Φ_f of **L** is less than 0.01. In these conditions, **L** is able to signal the presence of Zn(II) ion in solution while it does not respond to Cd(II). The behaviour towards Zn(II), agrees with the typical PET-regulated sensors in which the metal ion is coordinated by a polyamine functions linked to the fluorophore through a spacer; the diamagnetic close-shell of Zn(II) metal ion are able to prevent the PET effect engaging the amine lone pair in the coordination giving rise the Chelation Enhancement of Fluorescence effect (CHEF) and restoring the intrinsic

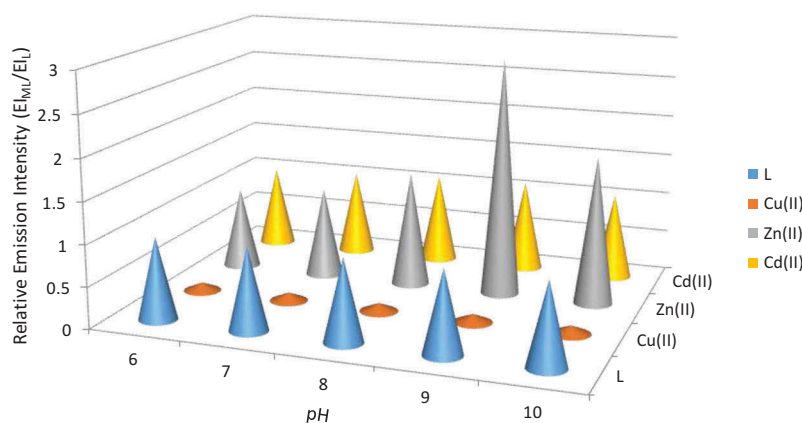


Figure 5. (Colour online) Schematic picture of the fluorescent response of **L** to Cu(II), Zn(II) and Cd(II) expressed as ratio between the emission intensities of 2M/**L** system and free **L** as a function of pH. [**L**] = $1.5 \cdot 10^{-5}$ mol·dm⁻³, [M(II)] = $3.0 \cdot 10^{-5}$ mol·dm⁻³, pH adjusted by adding HCl and NaOH aqueous solutions, $\lambda_{\text{ex}} = 280$ nm, $\lambda_{\text{em}} = 365$ nm.

fluorescence of the fluorophore without significant displacing of the emission wavelength maximum. This selective response to Zn(II) can be ascribed to the lower dimension of Zn(II) with respect to Cd(II) which allows it to better fit the polyamine coordination framework to be coordinated by all the four ammine functions while probably bigger Cd(II) ion does not.

Figure 6 reports the emission spectra for the titration of **L** in water/ethanol 99/1 with Zn(II) perchlorate as well as the emission trend as a function of the equivalents of Zn(II) added at pH = 9. Examining the trend of emission intensity at 365 nm by adding an increasing amount of Zn(II), three different zones, with two evident changes of slope, can be distinguished (Figure 6(b)). From 0 to 0.5 equivalents of Zn(II), the emission intensity slowly increased of the 11% with respect to the initial emission of the free **L**; from 0.5 to 1 equiv., the emission drastically increases reaching an increment of 65% with respect to that of free **L**. After the addition of one equivalent of Zn(II), the emission intensity proceeded to increase reaching the maximum at 2 equivalent with an increment of about 200% with respect to the initial emission of **L**; the successive addition of Zn(II) did not further affect the emission intensity that remains constant.

This emission behaviour can be justified assuming that by the addition of increasing amount of Zn(II) from 0 to 2 equivalents, different species having different **L** to Zn(II) stoichiometry form; three species can be hypothesised: the $[\text{ZnL}_2]^{2+}$, $[\text{ZnL}]^{2+}$, and $[\text{Zn}_2\text{L}]^{4+}$ species with the latter the more fluorescent.

This behaviour is different to that found with the chemosensor **L1**; first because **L1** resulted selective for Zn(II) at pH = 7.4 while **L** shift the fluorescent selective response to Zn(II) in the alkaline pH field; second because **L1** showed only mononuclear species with a 1:1 metal to ligand molar ratio while **L** exhibits complexes with

different stoichiometries. These differences can be ascribed to the different PPD or PPD-OMe sensing units. The presence of the two bulky methoxy groups limits the availability of the macrocyclic cavity as well as of the four ammine functions to the coordination of **L** with respect to **L1**. The bulk due to the OMe groups gives rise to **L**-metal complexes of lower stability at neutral pH, where protonated species exist for both **L** and **L1** systems, as well as to different stoichiometry ($[\text{CuL}_2]$ vs $[\text{CuL1}]$). In other words, while for **L1** the tetraamine fragment behaves as single binding unit this is not for **L**; in fact, two **L** species are necessary to stabilise Cu(II) at neutral pH, meaning that not all the amine functions of one **L** unit are involved in Cu(II) coordination as well as they are able to bind two Zn(II) ion at alkaline pH values.

Conclusion

The new macrocyclic ligand **L** (28,29-dimethoxy-27-oxa-8,11,14,17,25,26-hexaazatetracyclo[22.2.1.1(2,6).1(19,23)]nonacos-2,4,6(28),19,21,23(29),24,26(1)-octaene) has been synthesised. It contains a tetraamine chain as metal ions binding unit and the 2,5-bis(2-methoxy-3-methyl-phenyl)-1,3,4-oxadiazole as fluorescent sensing unit (PPD-OMe). **L** is soluble in water in the pH range of 2–12 and its fluorescent emission depends on the pH; it is highly fluorescent at low values of pH (pH = 2) while, the emission decreases increasing the pH. This behaviour is attributed to the PET effect generated by the amine functions taking place or not, depending on the protonation degree of the amines close to the PPD-OMe fluorophore.

The preliminary studies on the binding behaviour of **L** in aqueous solution towards selected metal ions by the **L** photochemical response were carried out.

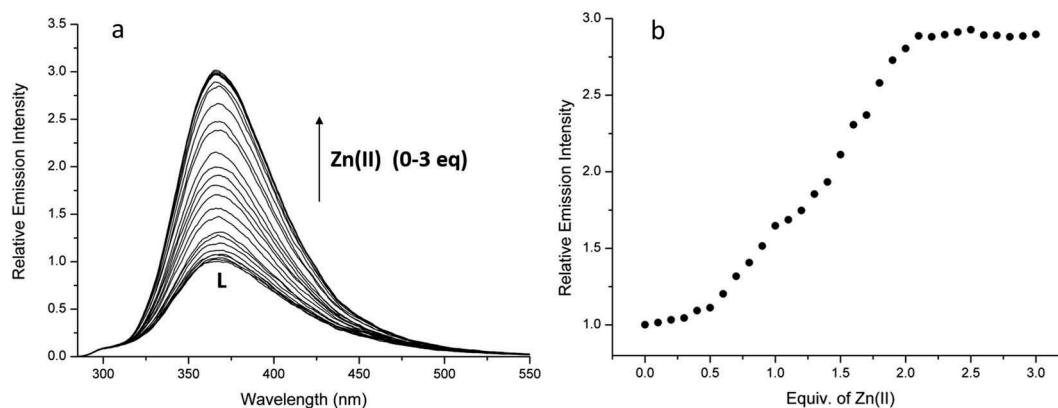


Figure 6. (a) Fluorescence spectra of **L** ($\lambda_{\text{ex}} = 280 \text{ nm}$) recorded in water/ethanol 99/1 v/v in the presence of CHES buffer ($10^{-3} \text{ mol}\cdot\text{dm}^{-3}$) at pH = 9.0 by adding $\text{Zn}(\text{ClO}_4)_2$. (b) Trend of the emission intensity ($\lambda_{\text{em}} = 365 \text{ nm}$) as a function of the equivalents of Zn(II) added. ($[\text{L}] = 1.5 \cdot 10^{-5} \text{ mol}\cdot\text{dm}^{-3}$).

The photochemical response of **L** in the presence of the transition metal ions Cu(II), Zn(II) and Cd(II) highlights that it is able to coordinate them by the tetraamine binding framework while the PPD-OMe fluorophore remains uninvolved in the coordination. The coordination of the metal ions affects the fluorescent emission that is perturbed differently depending on the pH. In particular, while the Cu(II) quenches the already low emission of **L** due to its is the coordination, Zn(II) switches on the emission. The best response for the presence of Zn(II) in solution occurs in the alkaline range of pH 7.5–10 with the maximum at pH about 9.

This is an interesting result allowing the determination of Zn(II) in a pH range often difficult to explore, mainly considering this from the biological point of view.

The presence of the two methoxy groups obstruct in part the macrocyclic cavity and so the tetraamine functions for the metal ion coordination; this reflects on the stoichiometry of the complexed species formed compared to similar macrocyclic ligands showing the same tetraamine fragment and different photochemical spacers. In this case, ligand to metal of 2:1 as well as of 1:2 stoichiometries were found, due probably to the lack of the contemporary involvement of the four amine functions in the metal ion coordination.

Further studies will be carried out to better investigate this aspect.

Acknowledgments

The authors thank the Italian Ministero dell'Istruzione dell'Università e della Ricerca (MIUR) project 2015MP34H3 and Department of Pure and Applied Sciences of the University of Urbino (project DISPEA_FORMICA_PROG17, DISPEA_FUSI_PROG17, DISPEA_GIORGI_PROG18).

Disclosure statement

No potential conflict of interest was reported by the authors.

Funding

This work was supported by the Ministero dell'Istruzione, dell'Università e della Ricerca [project 2015MP34H3].

References

- (1) Bissell, R.A.; De Silva, A.P.; Gunaratne, H.Q.N.; Lynch, P.L. M.; Maguire, G.E.M.; Sandanayake, K. *Chem. Soc. Rev.* **1992**, *21*, 187–195. DOI: [10.1039/CS9922100187](https://doi.org/10.1039/CS9922100187).
- (2) de Silva, A.P.; Fox, D.B.; Huxley, A.J.M.; Moody, T.S. *Coord. Chem. Rev.* **2000**, *205*, 41–57. DOI: [10.1016/S0010-8545\(00\)00238-1](https://doi.org/10.1016/S0010-8545(00)00238-1).

- (3) de Silva, A.P.; Gunaratne, H.Q.N.; Gunlaugsson, T.; Huxley, A.J.M.; McCoy, C.P.; Rademacher, J.T.; Rice, T.E. *Chem. Rev.* **1997**, *97*, 1515–66. DOI: [10.1021/cr960386p](https://doi.org/10.1021/cr960386p).
- (4) Prodi, L. *New J. Chem.* **2005**, *29*, 20–31. DOI: [10.1039/b411758a](https://doi.org/10.1039/b411758a).
- (5) Mayer, M.; Baeumner, A.J. *Chem. Rev.* **2019**, *119*, 7996–8027. DOI: [10.1021/acs.chemrev.8b00719](https://doi.org/10.1021/acs.chemrev.8b00719).
- (6) Singh, K.; Rotaru, A.M.; Beharry, A.A. *ACS Chem. Biol.* **2018**, *13*, 1785–1798.
- (7) Lvova, L.; Caroleo, F.; Garau, A.; Lippolis, V.; Giorgi, L.; Fusi, V.; Zaccheroni, N.; Lombardo, M.; Prodi, L.; Di Natale, C.; Paolesse, R. *Front.Chem.* **2018**, *6*, 1–10. DOI: [10.3389/fchem.2018.00110](https://doi.org/10.3389/fchem.2018.00110).
- (8) Desvergne, J.-P.; Czarnik, A.W. *Fluorescent Chemosensors of Ion and Molecule Recognition*, ed. NATO-ASI Series; Kluwer Academic Publishers, 1996.
- (9) Davis, F.; Collyer, S.D.; Higson, S.P.J. *Top. Curr. Chem.* **2005**, *255*, 97–124.
- (10) Jagt, R.B.C.; Kheibari, M.S.; Nitz, M. *Dyes Pigm.* **2009**, *81*, 161–165. DOI: [10.1016/j.dyepig.2008.10.003](https://doi.org/10.1016/j.dyepig.2008.10.003).
- (11) Zhang, Y.M.; Lin, Q.; Wei, T.B.; Wang, D.D.; Yao, H.; Wang, Y.L. *Sensor Actuat.B-Chem.* **2009**, *137*, 447–455. DOI: [10.1016/j.snb.2009.01.015](https://doi.org/10.1016/j.snb.2009.01.015).
- (12) Kim, U.I.; Suk, J.M.; Naidu, V.R.; Jeong, K.S. *Chem. Eur. J.* **2008**, *14*, 11406–11414.
- (13) Gale, P.A. *Chem. Commun.* **2008**, 4525–4540.
- (14) Schazmann, B.; Alhashimy, N.; Diamond, D. *J. Am. Chem. Soc.* **2006**, *128*, 8607–8614. DOI: [10.1021/ja061917m](https://doi.org/10.1021/ja061917m).
- (15) Lakowicz, J.R. *Principles of Fluorescence Spectroscopy*; Kluwer Academic/Plenum Publishers, New York, 1999.
- (16) Valeur, B.; Leray, I. *Coord. Chem. Rev.* **2000**, *205*, 3–40. DOI: [10.1016/S0010-8545\(00\)00246-0](https://doi.org/10.1016/S0010-8545(00)00246-0).
- (17) Lodeiro, C.; Capelo, J.L.; Mejuto, J.C.; Oliveira, E.; Santos, H.M.; Pedras, B.; Nunez, C. *Chem. Soc. Rev.* **2010**, *39*, 2948–76. DOI: [10.1039/b819787n](https://doi.org/10.1039/b819787n).
- (18) Formica, M.; Fusi, V.; Giorgi, L.; Micheloni, M. *Coord. Chem. Rev.* **2012**, *256*, 170–92. DOI: [10.1016/j.ccr.2011.09.010](https://doi.org/10.1016/j.ccr.2011.09.010).
- (19) (a) Van Wouwe, J.P. *Eur. J. Pediatr.* **1989**, *149*, 2–8; (b) Cousins, R.I. *Present Knowledge in Nutrition*; Zeigler, E.E., Filer L.J. Eds.; ILSI Press: Washington, DC, 1996. (c) Tubek, S.; Grzanka, P.; Tubek, I. *Biol. Trace Elem. Res.* **2008**, *121*, 1–8. (d) Krezel, A.; Maret, W. *Arch. Biochem. Biophys.* **2016**, *611*, 3–19. (e) Frederickson, C.J.; Koh, J.Y.; Bush, A.I. *Nat. Rev. Neurosci.* **2005**, *6*, 449–462. (f) Berg, J.M.; Shi, Y. *Science* **1996**, *271*, 1081–1085. (g) O'Halloran, T.V. *Science* **1993**, *261*, 715–725. DOI: [10.1007/BF02024322](https://doi.org/10.1007/BF02024322).
- (20) (a) Maret, W. *Metallomics* **2015**, *7*, 202–211; (b) Nolan, E. M.; Lippard, S.J. *Acc. Chem. Res.* **2009**, *42*, 193–203. DOI: [10.1039/C4MT00230J](https://doi.org/10.1039/C4MT00230J).
- (21) (a) Lindskog, S. *Pharmacol. Ther.* **1997**, *74*, 1–20; (b) Silverman, D.N.; Lindskog, S. *Acc. Chem. Res.* **1988**, *21*, 30–36. DOI: [10.1016/S0163-7258\(96\)00198-2](https://doi.org/10.1016/S0163-7258(96)00198-2).
- (22) (a) Nair, S.K.; Christianson, D.W. *J. Am. Chem. Soc.* **1991**, *113*, 9455–9458; (b) Fisher, Z.; Hernandez Prada, J.A.; Tu, C.; Duda, D.; Yoshioka, C.; An, H. *Biochemistry* **2005**, *44*, 1097–1105. DOI: [10.1021/ja00025a005](https://doi.org/10.1021/ja00025a005).
- (23) (a) Formica, M.; Fusi, V.; Paoli, P.; Piersanti, G.; Rossi, P.; Zappia, G.; Orlando, P. *New J. Chem.* **2008**, *32*, 1204–1214; (b) Ambrosi, G.; Formica, M.; Fusi, V.; Giorgi, L.; Macedi, E.; Piersanti, G.; Retini, M.; Varrese, M.A.; Zappia, G. *Tetrahedron* **2012**, *68*, 3768–3775. (c)

- Amatori, S.; Ambrosi, G.; Borgogelli, E.; Fanelli, M.; Formica, M.; Fusi, V.; Giorgi, L.; Macedi, E.; Micheloni, M.; Paoli, P.; Rossi, P.; Tassoni, A. *Inorg. Chem.* **2014**, *53*, 4560–4569. (d) Formica, M.; Fusi, V.; Giorgi, L.; Piersanti, G.; Retini, M.; Zappia, G. *Tetrahedron* **2016**, *72*, 7039–7049. DOI: [10.1039/b719342d](https://doi.org/10.1039/b719342d).
- (24) (a) Ambrosi, G.; Ciattini, S.; Formica, M.; Fusi, V.; Giorgi, L.; Macedi, E.; Micheloni, M.; Paoli, P.; Rossi, P.; Zappia, G. *Chem. Commun.* **2009**, 7039–7041; (b) Amatori, S.; Ambrosi, G.; Fanelli, M.; Formica, M.; Fusi, V.; Giorgi, L.; Macedi, E.; Micheloni, M.; Paoli, P.; Pontellini, R.; Rossi, P. *Chem. Eur. J.* **2012**, *18*, 4274–4284. (c) Arca, M.; Caltagirone, C.; De Filippo, G.; Formica, M.; Fusi, V.; Giorgi, L.; Lippolis, V.; Prodi, L.; Rampazzo, E.; Scorciapino, M.A.; Sgarzi, M.; Zaccheroni, N. *Chem. Commun.* **2014**, *50*, 15259–15262. doi:[10.1039/b913435b](https://doi.org/10.1039/b913435b)
- (25) (a) Formica, M.; Favi, G.; Fusi, V.; Giorgi, L.; Mantellini, F.; Micheloni, M. *J. Lumin.* **2018**, *195*, 193–200; (b) Ambrosi, G.; Formica, M.; Fusi, V.; Giorgi, L.; Macedi, E.; Micheloni, M.; Paoli, P.; Rossi, P. *Inorg. Chem.* **2016**, *55*, 7676–7687. (c) Ambrosi, G.; Formica, M.; Fusi, V.; Giorgi, L.; Macedi, E.; Micheloni, M.; Paoli, P.; Pontellini, R.; Rossi, P. *Chem. Eur. J.* **2011**, *17*, 1670–1682. DOI: [10.1016/j.jlumin.2017.11.018](https://doi.org/10.1016/j.jlumin.2017.11.018).
- (26) (a) Ambrosi, G.; Formica, M.; Fusi, V.; Giorgi, L.; Macedi, E.; Micheloni, M.; Piersanti, G.; Pontellini, R. *Org. Biomol. Chem.* **2010**, *8*, 1471–1478; (b) Fusi, V.; Giorgi, L.; Formica, M.; Micheloni, M.; Macedi, E.; Ambrosi, G.; Paoli, P.; Rossi, P.; Pontellini, R. *Inorg. Chem.* **2010**, *49*, 9940–9948. (c) Terenzi, A.; Fanelli, M.; Ambrosi, G.; Amatori, S.; Fusi, V.; Giorgi, L.; Turco Liveri, V.; Barone, G. *Dalton Trans.* **2012**, *41*, 4389–4395. DOI: [10.1039/b921053a](https://doi.org/10.1039/b921053a).
- (27) (a) Chhama, S.; Sanchit, S. *J. Drug Deliv. Ther.* **2015**, *5*, 8–13; (b) Khalil, N.A.; Kamal, A.M.; Emam, S.H. *Biol. Pharm. Bull.* **2015**, *38*, 763–773. (c) Patel, N.B.; Purohit, A.C.; Rajani, D.P.; Moo-Puc, R.; Rivera, G. *Eur. J. Med. Chem.* **2013**, *62*, 677–687. (d) Rapolu, S.; Alla, M.; Bommena, V. R.; Murthy, R.; Jain, N.; Bommareddy, V.R.; Bommineni, M. R. *Eur. J. Med. Chem.* **2013**, *66*, 91–100.
- (28) (a) Homocianu, M.; Airinei, A. *J. Fluoresc.* **2016**, *26*, 1617–1635; (b) Wen, S.; Pei, J.; Zhou, Y.; Xue, L.; Xu, B.; Li, Y.; Xu, B.; Tian, W. *J. Polym. Sci. Part A Polym. Chem.* **2009**, *47*, 1003–1012. (c) Schab-Balcerzak, E.; Grucela-Zajac, M.; Krompiec, M.; Janeczek, H.; Siwy, M.; Sek, D. *Synth. Met.* **2011**, *161*, 2268–2279. (d) Kulkarni, A.P.; Tonzola, C.J.; Babel, A.; Jenekhe, S.A. *Chem. Mater.* **2004**, *16*, 4556–4573. DOI: [10.1007/s10895-016-1848-6](https://doi.org/10.1007/s10895-016-1848-6).
- (29) (a) Formica, M.; Ambrosi, G.; Fusi, V.; Giorgi, L.; Arca, M.; Garau, A.; Pintus, A.; Lippolis, V. *New J. Chem.* **2018**, *42*, 7869–7883; (b) Paoli, P.; Rossi, P.; Ambrosi, G.; Formica, M.; Fusi, V.; Giorgi, L.; Micheloni, M.; Macedi, E. *Supramol. Chem.* **2017**, *29*, 896–911. (c) Amatori, S.; Ambrosi, G.; Errico Provenzano, E.; Fanelli, M.; Formica, M.; Fusi, V.; Giorgi, L.; Macedi, E.; Micheloni, M.; Paoli, P.; Rossi, P. *J. Inorg. Biochem.* **2016**, *162*, 154–161. (d) Ambrosi, G.; Borgogelli, E.; Formica, M.; Fusi, V.; Giorgi, L.; Micheloni, M.; Rampazzo, E.; Sgarzi, M.; Zaccheroni, N.; Prodi, L. *Sens. Act., B* **2015**, *207*, 1035–1044. DOI: [10.1039/C8NJ00113H](https://doi.org/10.1039/C8NJ00113H).
- (30) Bencini, A.; Burguete, M.I.; Garcia-España, E.; Luis, S.V.; Miravet, J.F.; Soriano, C. *J. Org. Chem.* **1993**, *58*, 4749–4753. DOI: [10.1021/jo00069a049](https://doi.org/10.1021/jo00069a049).
- (31) Jyotirmayee, M.; Pal, H.; Sapre, A.V. *Bull. Chem. Soc. Jpn.* **1999**, *72*, 2193–2202.
- (32) Mashraqui, S.H.; Sundaram, S.; Khan, T.; Bhasikuttan, A.C. *Tetrahedron* **2007**, *63*, 11093–11100.
- (33) Richman, J.E.; Atkins, T.J. *J. Am. Chem. Soc.* **1974**, *96*, 2268–2270. DOI: [10.1021/ja00814a056](https://doi.org/10.1021/ja00814a056).
- (34) Czarnik, A.W. *Fluorescent Chemosensor for Ion and Molecule Recognition*; American Chemical Society: Washington, DC, **1993**.